Spectrochimica Acta Part A: Molecular and Biomolecular Spectroscopy 164 (2016) 1–7

Contents lists available at ScienceDirect

Spectrochimica Acta Part A: Molecular and Biomolecular Spectroscopy

journal homepage: www.elsevier.com/locate/saa

Electronic, structural and vibrational induced effects upon ionization of 2-quinolinone

A. Bellili [a], Y. Pan [b], M.M. Al Mogren [c], K.C. Lau [b,*], M. Hochlaf [a,*]

[a] Université Paris-Est, Laboratoire Modélisation et Simulation Multi Echelle, MSME UMR 8208 CNRS, 5 bd Descartes, 77454 Marne-la-Vallée, France
[b] Department of Biology and Chemistry, City University of Hong Kong, Kowloon, Hong Kong
[c] Chemistry Department, Faculty of Science, King Saud University, PO Box 2455, Riyadh 11451, Saudi Arabia

ARTICLE INFO

Article history:
Received 13 January 2016
Received in revised form 22 March 2016
Accepted 27 March 2016
Available online 6 April 2016

Keywords:
2-Quinolone cation
Electronic states
Ab initio computations
Ionization energies
DNA analogs

ABSTRACT

Using first principle methodologies, we characterize the lowest electronic states of 2-quinolinone$^+$ cation. The ground state of this ion is of $\tilde{X}^2A''$ nature. We deduce the adiabatic ionization energy of 2-quinolinone to be equal 8.249 eV using the explicitly correlated coupled cluster level and where zero point vibrational energy, core-valence and scalar relativistic effects are taken into account. We examine also the ionization induced structural changes and vibrational shifts and analyze the electron density differences between the neutral and ionic species. These data show that the formation of 2-quinolinone$^+$ $\tilde{X}^2A''$ from 2-quinolinone affects strongly the HNCO group, whereas the carbon skeletal is perturbed when the upper electronic cationic states are populated. The comparison to 2-pyridone allows the elucidation of the effect of benzene ring fused with this heterocyclic ring. Since quinolones and pyridones are both model systems of DNA bases, these findings might help in understanding the charge redistribution in these biological entities upon ionization.

1. Introduction

Quinolones form a class of molecules, which contain a benzene ring fused with a heterocyclic ring of 2-pyridone. Since their discovery (>50 years ago), they are used as chemical antimicrobial agents. They are naturally produced by some plants, animals and bacteria or synthetized in laboratory. They possess a wide range of applications as antimicrobials and/or signaling activities molecules [1–4]. Synthesis of such compounds and the investigation of their medical and pharmacological properties is still an active field [5]. These works aim at understanding the action mechanisms of quinolones against pathogenic bacteria and the induced microorganism resistance and toxicity in treated patients. Nevertheless, some secondary effects of quinolones are not under control. For instance, these agents elicit photosensitivity as a side effect but their interaction, at the molecular level, with light and especially ionizing light is not known [6]. Therefore, the investigation of the spectroscopic and electronic properties of these molecules and their ionic forms is mandatory to understand their roles for further medical and pharmacological applications and developments.

Recently, we performed a detailed theoretical study on the neutral 2-quinolone (Fig. 1) [7], in which we determined the equilibrium geometries and the vibrational structure of the keto form (lactam) and the enol form (lactim). The focus was also on the tautomerism and the electronic excited states of these species. We confirmed hence that the lactam form, 2-quinolinone (keto, denoted as 2Q) is more stable (by ~0.1 eV) than the lactim form, 2-hydroxyquinoline (enol, denoted as 2HQ) in gas phase as it is also the case in condensed phases [8–12].

At present we examine the cationic form of 2-quinolone (denoted hereafter as 2Q$^+$) using density functional theory (DFT) and *ab initio* methodologies. In contrast to the neutral 2Q molecule, the data on 2Q$^+$ are scarce. Most of them are limited to the earlier photoelectron spectroscopic study by Pfister-Guillouzo et al. [13]. These authors identified in their PES spectrum six bands in the 8–13 eV energy range. These bands were assigned to the population of the lowest electronic states of 2Q$^+$ and/or to its tautomeric forms. Indeed, the authors were unable to confidently assign the measured vertical ionization energies to the 2Q species. In this contribution, we deeply investigate the 2Q$^+$ cation that may be formed after ionizing the corresponding neutral molecule. In Ref. [7], we showed that the keto-enol barrier for the neutral species is quite high (>1.5 eV) so that we can consider 2-quinolinone solely for its ionization. Specifically, we compute the equilibrium geometries and the vibrational structure of 2Q$^+$ and the pattern of its lowest electronic states. Also, we deduce the adiabatic and vertical ionization energies of 2Q. Moreover, we perform an analysis of the molecular orbitals (MOs) of neutrals 2-pyridone (2PY) and 2Q and the electron densities differences between their neutral and ionic species in order to elucidate the effect of annelation on 2PY and the charge redistribution upon ionization with and without the additional benzene ring in 2Q. These features are important to understand these effects on DNA

* Corresponding authors.
E-mail addresses: kaichung@cityu.edu.hk (K.C. Lau), hochlaf@univ-mlv.fr (M. Hochlaf).

http://dx.doi.org/10.1016/j.saa.2016.03.043
1386-1425/

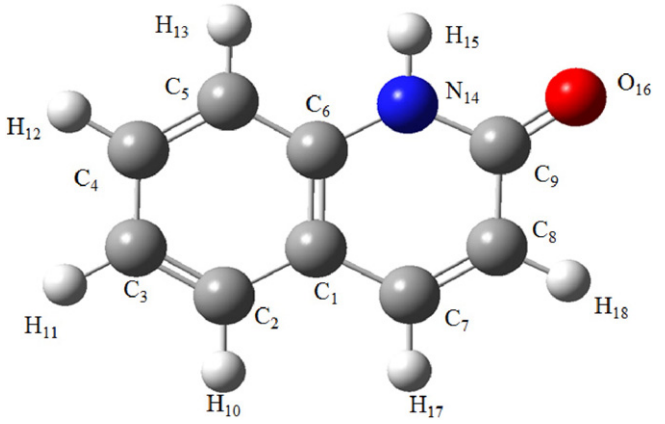

Fig. 1. Equilibrium structure of the ground state of singlet 2-quinolinone ($\tilde{X}^1A'$, 2Q). The numbering of the atoms used in the tables is also given.

bases since both quinolones and pyridones are considered as model systems of these biological entities [14].

2. Methodologies

The electronic structure computations on the ionic $2Q^+$ are carried out using the GAUSSIAN09 [15] and MOLPRO (Version 2010.1) [16] suites of programs. The computations concern the equilibrium geometries and vibrational spectroscopy of the lowest doublet states of $2Q^+$ and their pattern. These optimizations are done, in the C_1 point group, using the PBE0 [17,18] density functional (using the ultrafine integral grids) and the complete active-space self-consistent field (CASSCF) [19,20] levels as implemented in GAUSSIAN09 and MOLPRO, respectively. The default options were used. The CASSCF active space (in C_s point group) comprised a set of 26a′ + 8a″ valence orbitals (active) and 11a′ core orbitals (frozen). Out of the 26a′ + 8a″ valence orbitals, the first 18a′ + 3a″ valence orbitals were kept as closed orbitals. This results in ~4.9×10^5 configuration state functions (CSFs) to be considered. Several tests were performed to determine the appropriate size of active space without significant change in the order of electronic states of the $2Q^+$ in the 0–7 eV internal energy domain. Furthermore, we used the state-averaged CASSCF technique followed by the internally contracted multi-reference configuration interaction (MRCI) approach [21–23] to compute the pattern of the lowest doublet electronic states of $2Q^+$. For MRCI, all configurations with coefficients larger than 0.5 in the CI expansion of the CASSCF wave functions were used as a reference and seven more a′ valence orbitals were frozen. This leads to ~1.2×10^8 uncontracted configurations to be treated in the cations. For better accuracy we considered the Davidson corrected MRCI (MRCI + Q) energies [24]. Here the atoms were described using the aug-cc-pVXZ (X = D, T) or the 6-311G(d,p) basis sets [25–28]. The anharmonic frequencies at the PBE0/aug-cc-pVDZ levels were obtained from the derivatives (second, third, and fourth) of the ground state potentials and second-order perturbation theory treatment of nuclear motions as implemented in GAUSSIAN 09 [15]. The scaling factors for harmonic frequencies at the PBE0/aug-cc-pVTZ and CASSCF levels are 0.9579 and 0.91, respectively.

To predict accurately the ionization energy of 2Q, we employed the explicitly correlated coupled clusters method with perturbative treatment of triple excitations (*i.e.* (R)CCSD(T)-F12 (approximation B)) [29–31]. Within the explicitly correlated computations, the atoms were described using the cc-pVTZ-F12 explicitly correlated basis sets [32], in conjunction with the corresponding auxiliary basis sets, density fitting functions [33–35] and the default CABS(OptRI) basis sets of Yousaf and Peterson [36]. We also considered the core-valence (CV) and scalar-relativistic (SR) effects: CV effects are deduced as the difference between electronic energies with only valence electrons correlated and that with both core and valence electrons correlated at the (R)CCSD(T)/cc-pwCVTZ level of theory [37,38]. The core electrons are the 1*s* electrons of carbon, nitrogen, and oxygen. The SR energetic contributions are taken as the difference between electronic energies at the (R)CCSD(T)/cc-pVTZ level [39–42] without using the spin-free, one-electron Douglas-Kroll-Hess (DKH) Hamiltonian [43,44] and at the (R)CCSD(T)/cc-pVTZ-DK level [45] with the DKH Hamiltonian. These computations are done using MOLPRO.

3. Characterization of the lowest electronic states of $2Q^+$

The dominant electronic configuration of 2Q is $(30a')^2(31a')^2(32a')^2(4a'')^2(5a'')^2(6a'')^2$ [7]. The electronic ground state $\tilde{X}^2A''$ of $2Q^+$ is obtained after removal of an electron from the outermost (6a″) molecular orbital (MO) of 2Q. As shown in Fig. 2, the (6a′) MO is π in nature and spreads over both rings.

The PBE0/aug-cc-pVXZ (X = D, T) optimized equilibrium structures of 2Q and of $2Q^+$ are given in Table 1. We also show the structure obtained at the CASSCF/6-311G(d,p) level. Both PBE0/aug-cc-pVTZ and CASSCF/6-311G(d,p) are close to each other, whereas some deviations, mainly on the parameters relative to the HNCO group, are observed when using PBE0 with the aug-cc-pVDZ basis set. In the following, we will rely on the data obtained using the larger basis sets.

As for $2Q(\tilde{X}^1A')$, we found a planar equilibrium structure for $2Q^+(\tilde{X}^2A'')$. Upon ionization, the main changes between 2Q ($\tilde{X}^1A'$) and $2Q^+$ ($\tilde{X}^2A''$) concern the bond lengths of N_{14}—C_6 and C_6—C_1, and the bond angles of N_{14}—C_9—O_{16}, C_8—C_9—O_{16} and N_{14}—C_9—C_8. The bond lengths of N_{14}—C_9, C_3—C_4, and C_5—C_6 are also altered by about 0.04 Å. More generally, these distances and angles vary by ~0.04–0.08 Å and 2°–4° upon ionizing 2Q. These changes are relatively small. Based on the Franck-Condon principle, we expect hence that the $2Q(\tilde{X}^1A') + h\nu \rightarrow 2Q^+(\tilde{X}^2A'') + e^-$ photoionization transition is associated with a long vibrational progression dominated by the $\tilde{X}0_0^0$ transition. In order to go further, one needs to compute the Franck-Condon factors (FCFs) for the $2Q(X^1A') + h\nu \rightarrow 2Q^+ + e^-$ process using, for instance, the procedure described recently by Palmer et al. [46].

The first electronic excited state $2^2A''$ of $2Q^+$ is located at ~1.2 eV above $2Q^+(\tilde{X}^2A'')$. It is obtained after removal of an electron from the (5a″) MO of 2Q. Fig. 2 shows that this MO has a π character and it is localized mainly on the benzene ring of 2Q with a small contribution from the HNCO group. We used the SA-CASSCF procedure to optimize the equilibrium geometry and obtain the vibrational structure of $2Q^+(2^2A'')$. The corresponding data are listed in Table 1. The comparison between the structure of $2Q^+(2^2A'')$ and that of $2Q(\tilde{X}^1A')$ reveals that both species have quite similar equilibrium geometries. Indeed, the main geometrical differences between the $2Q(\tilde{X}^1A')$ and $2Q^+(2^2A'')$ are the N_{14}—C_6, N_{14}—C_9 bond lengths and the C—C bonds within the benzene ring. We expect hence population of the corresponding stretching modes during the photoionization transition of $2Q(\tilde{X}^1A') + h\nu \rightarrow 2Q^+(2^2A'') + e^-$. Similar to the ground state, the $2^2A''0_0^0$ band should have appreciable intensity in the experimental spectra.

Table 2 lists the dominant electron configurations and vertical excitation energies of the lowest doublet states of $2Q^+$. These energies are computed at the equilibrium geometry of $2Q^+(\tilde{X}^2A'')$ using CASSCF, MRCI and MRCI + Q methods. In the following, we will quote the MRCI + Q energies as they are expected to be the most reliable ones. The $1^2A'$ state is located at ~1.54 eV (Table 2). The $1^2A'$ state is obtained after removal of one electron from the (32a′) MO (Fig. 2). Then, we compute two closely lying states: the $3^2A''$ state at ~3.50 eV and the $4^2A''$ state at 4.20 eV. Above 5 eV, a high density of electronic states is